

36p

NO 14806

NASA TN D-1770

Code 1



# TECHNICAL NOTE

D-1770

SOME POSSIBILITIES FOR DETERMINING THE CHARACTERISTICS  
OF THE ATMOSPHERES OF MARS AND VENUS FROM  
GAS-DYNAMIC BEHAVIOR OF A PROBE VEHICLE

By Alvin Seiff

Ames Research Center  
Moffett Field, Calif.

NATIONAL AERONAUTICS AND SPACE ADMINISTRATION  
WASHINGTON

April 1963

Code

NATIONAL AERONAUTICS AND SPACE ADMINISTRATION

---

TECHNICAL NOTE D-1770

---

SOME POSSIBILITIES FOR DETERMINING THE CHARACTERISTICS  
OF THE ATMOSPHERES OF MARS AND VENUS FROM  
GAS-DYNAMIC BEHAVIOR OF A PROBE VEHICLE

By Alvin Seiff

SUMMARY

14806

One of the early objectives of space probes sent to Mars and Venus will be to determine the characteristics of the atmospheres on those planets for scientific purposes. Characteristics of interest include profiles of gas density, temperature, and pressure above the planet surface, and chemical composition of the atmosphere. Because of practical limitations, it is doubtful that the first probes will convey a very complete picture of the atmosphere, and a good initial objective will be to define the above properties broadly, although certainly the more that can be learned from an early probe the better.

So far, the entry probe has been considered merely a vehicle for delivering instruments to planets, and the interactions of the probe with the atmosphere have been considered problems to be overcome if the mission is to be accomplished. The present paper is based on the premise that these interactions are a fertile source of information about the atmosphere. The development of this premise suggests some experiments which are simple (and therefore it is hoped reliable), lightweight, and productive of valuable information on the planets' atmospheres.

It is found that the density, pressure, and  $RT$  product profiles in the atmosphere can be obtained from measurements of axial acceleration and the angle of entry into the atmosphere. For a certain class of entry body configurations, measurements of the static flight stability can be used to give information on the mean ratio of specific heats of the atmospheric gases. Measuring the ambient temperature so as to obtain the gas constant  $R$  from its product with temperature,  $RT$ , and hence determine the mean molecular weight of the atmospheric gases is discussed. Luminosity detectors that view the excited high-temperature gases in the probe shock layer for evidence of composition are discussed as well as the possibility of determining the kind of gases from measurements of stagnation temperatures.

An important characteristic of this kind of probe experiment is that the definition of atmospheric properties begins as high in the atmosphere as any detectable effect on the probe occurs - in general, around 300,000 feet altitude.

## INTRODUCTION

One of the early objectives of the exploration of Mars and Venus by space probes will almost certainly be to determine the composition, pressure, density, and temperature profiles of their surrounding atmospheres. Not only is this information of scientific interest for what it can indicate about the nature of the planet, its evolutionary state, and the possibilities of supporting life but it is also essential for the proper design of subsequent, more advanced entry vehicles.

The constraints under which this exploration must be accomplished are as follows. The initial instrument payload weights will be small because of booster limitations. The communications problem is difficult because of the large distance to earth and the limited power available on the vehicle. The reliability requirement is severe since the instruments and communications equipment must remain in operable condition from 10 to 40 weeks during interplanetary transit, and then function perfectly for a brief period during which the mechanical loading and heating may be severe. These constraints suggest that the best possibility of success lies in the choice of simple instruments and passive systems. Elegant and complicated equipment may give promise of defining the atmospheric environment precisely and in great detail, but is incompatible with small size and weight, simple communication, and long-term reliability.

In the design of the entry probe vehicle, numerous problems arising from the interaction of the vehicle with the atmosphere must be treated. These include the capsule flight stability, the aerodynamic heating, both radiative and convective, and the determination of the flight trajectory. The designer, preoccupied with the solution of these problems and hampered by uncertainty in the nature of the atmosphere to be entered, is inclined to view them as obstacles to the fulfillment of the mission. However, one may also view the vehicle interactions with the atmosphere as a primary source of data about the nature of the atmosphere. As a simple example previously considered for application in the earth's atmosphere, the deceleration of the vehicle combined with a known drag coefficient and speed will give the atmospheric density. There are other similar possibilities which, if compatible with the requirements of simplicity, reliability, and low weight (and, in the author's opinion, they tend to be), should perhaps be seriously contemplated for the early probe missions.

In this report, a number of possible ways in which interactions of a probe with the atmosphere can lead to knowledge of the atmosphere are described. Methods are included for experimentally determining atmospheric density, pressure, and RT product profiles, mean ratio of specific heats, ambient temperature, mean molecular weight of the atmospheric gases, and percentage of carbon dioxide in mixtures of carbon dioxide and nitrogen. The emphasis is on concepts and principles. No attempt is made to evaluate the relative merit of the experiments described, although it is certain that some of the measurements described will be found to be simpler, or more useful, or more feasible than others. Without further detailed engineering and scientific study, however, it is not possible to say conclusively what the relative merits are. The principal purpose of the present paper is to put these techniques for planetary atmospheric research before the interested reader.

# NOTATION

a	speed of sound
a <sub>x</sub>	acceleration in flight direction
A	reference area for gas-dynamic coefficients
B	ballistic constant, $\frac{C_D A}{m} \frac{\rho_0}{\beta \sin \theta}$
C <sub>D</sub>	drag coefficient, $\frac{\text{drag force}}{(1/2)\rho_\infty V^2 A}$
C <sub>m</sub>	static-stability coefficient, $\frac{\text{restoring moment}}{(1/2)\rho_\infty V^2 A d}$
C <sub>m<math>\alpha</math></sub>	static-stability derivative, $\frac{dC_m}{d\alpha}$
C <sub>m<math>\alpha</math>i</sub>	static-stability derivative at $\alpha = 0$
C <sub>p</sub>	pressure coefficient, $\frac{p - p_\infty}{(1/2)\rho_\infty V^2}$
d	reference length for gas-dynamic coefficients
D	acceleration profile function (appendix A)
f	frequency of pitching oscillation
F	frequency constant characteristic of probe (appendix A)
g	gravitational acceleration within the atmosphere of the planet under exploration
h	altitude above planet surface
h <sub>s</sub>	stagnation-point enthalpy of the flow
I	moment of inertia about transverse axis through center of gravity
m	vehicle mass
M	flight Mach number, $\frac{V}{a_\infty}$
M.W.	molecular weight of atmospheric gas mixture
p	static pressure
R	gas constant for atmospheric gas mixture, $\frac{p}{\rho T}$

$R_u$	universal gas constant, $R \times \text{M.W.}$
$t$	time
$T$	gas temperature
$V$	flight velocity
$W$	vehicle weight on earth
$\alpha$	angle of attack, angle between vehicle axis and flight direction
$\beta$	reciprocal of atmospheric scale height, $\frac{g}{RT}$
$\gamma$	ratio of specific heats of atmospheric gas mixture
$\rho$	gas density
$\sigma$	radius of gyration of probe about a transverse axis through the center of gravity
$\theta$	flight-path angle measured relative to horizontal
$\xi$	gas-dynamic damping coefficient (appendix A)

#### Subscripts

$\infty$	ambient conditions in undisturbed atmosphere
$e$	earth reference values
$E$	conditions at entry into the atmosphere
$s$	at the flow stagnation point
$o$	at the planet surface
$u$	upper portion of the atmosphere
$l$	lower portion of the atmosphere

## EXPERIMENTS BASED ON ENTRY BODY DYNAMICS

### Atmospheric Density

The density of a planet's atmosphere may, in principle, be determined for any instant of flight from a measurement of the deceleration. The governing equation is simply Newton's second law of motion with the defining equation for the drag coefficient representing the drag force.

$$C_D \frac{1}{2} \rho V^2 A = -m \frac{dV}{dt} \quad (1a)$$

or

$$\rho = - \frac{2dV/dt}{V^2 C_D A / m} \quad (1b)$$

The mass and frontal area of the entry vehicle are known prior to flight, and the velocity must be determined. The velocity at entry is obtainable from deep-space trajectory data provided by tracking and machine computation. The velocity after entry may be determined from integration of the accelerometer output. If the measurement is restricted to altitudes where continuum flow occurs, and this is expected to be the greatest part of the atmosphere, the drag coefficient may be considered known. Experimental facilities on earth are capable of defining the drag coefficient for wide ranges of speed, Reynolds number and attitude, and for various gases. Presently available experimental data (ref. 1) indicate that the drag coefficients of several types of entry bodies are insensitive to the composition of the atmospheres through which they fly. Hence the accuracy of the determination should not be seriously limited by present uncertainty in the composition of the planets' atmospheres. However, if the composition could be determined better from other results of a probe flight or from other experiments, the drag coefficient for the proper gaseous environment would then be measured in ground facilities.

The effect of angle-of-attack oscillations on the measurement could be significant. Since the accelerometer would most conveniently measure the axial force rather than the drag, and since the axial force tends in general to diminish with increasing angle of attack, a proper interpretation of the data would require angle-of-attack sensors in the probe. These are desired for another reason as well, and will be discussed in a later section.

The principal limitation on accuracy of the measurement of density would probably be in determining the velocity from accelerometer data. The accelerometer should be able to sense accelerations over a tenfold range with an accuracy of the order of 1 percent of the reading. This accuracy is required because the output of the accelerometer must be integrated to obtain the velocity. If measurements are continued to the time when  $V/V_E = 0.1$ , if the error in measured acceleration is systematic and constant at 1 percent of the reading, and if there is also a 1-percent error in  $V_E$  which adds to the other error, then the error in density will increase as the entry progresses and will reach a maximum of approximately 40 percent. The following table shows some accuracies calculated for these hypothetical conditions, as a function of the instantaneous flight

velocity ratio.

<u>V/V<sub>E</sub></u>	<u>Percent error in <math>\rho</math></u>
1.0	3
.8	4
.5	7
.2	20
.1	40

The altitudes at which these velocity ratios are obtained will be considered in a later section. It is evident that an accurate accelerometer is needed to maintain accuracy in density throughout the entry.

An alternative way of measuring atmospheric density at high vehicle velocities is by means of the pitot pressure. The pitot pressure coefficient is defined by

$$C_{ps} = \frac{p_s - p_\infty}{(1/2)\rho_\infty V^2} \quad (2)$$

where  $p_s$  is the pressure recorded at a stagnation-point orifice and  $p_\infty$  is the ambient pressure in the free stream. At high speeds,  $p_\infty$  may be neglected, having values about one-thousandth of  $p_s$ . Hence the pitot-pressure equation may be simplified and solved for the density to obtain

$$\rho = \frac{2p_s}{C_{ps} V^2} \quad (3)$$

Thus the ambient density is defined by a pressure measurement, given the velocity and the coefficient  $C_{ps}$ . (It will be noted, however, that the accelerometer is still required to provide the velocity history.)

The pitot-pressure coefficient, like the drag coefficients of blunt bodies, is insensitive to gas composition at high speeds. The limiting value given by Newtonian theory, 2, represents the condition of total streamwise momentum loss at the bow wave and is a good approximation at high speeds for both ideal and real gases. In the following table, theoretical values of  $C_{ps}$  are given for various gases, characterized by different values of the ratio of specific heats, and for various speeds.

<u><math>\gamma</math></u>	<u>M</u>	<u><math>C_{ps}</math></u>
1.40	5	1.81
1.40	$\infty$	1.85
1.67	$\infty$	1.76
1.00	$\infty$	2.00
Real air	> 10	1.9



It is apparent that a value of 1.90, selected without knowledge of the gas composition, would be correct within 5 percent; and this would be subject to iterative improvement from straightforward real-gas computations, given a composition of the atmosphere.

It may be remarked that a measurement of the pitot pressure is essentially a measurement of the local drag in the neighborhood of the stagnation point; and that it does not differ in principle from the measurement of drag as a way of determining ambient density. Pressure measurements at other locations of the orifice - not at a stagnation point - can also be used to obtain free-stream density, provided the local pressure coefficient is known. For example, pressure orifices could be used on cones with attached bow waves. The orifice location should in any case be chosen so that the measured pressures will be large compared to free-stream pressure, to minimize the error introduced by taking the difference,  $p - p_\infty$ , in the numerator of equation (2).

#### Atmospheric Pressure and RT Product

From a measured history of density as a function of time, the local static pressure may be deduced with the aid of the barometric equation

$$\frac{1}{T} \frac{dT}{dh} + \frac{1}{\rho} \frac{d\rho}{dh} = - \frac{g}{RT} \quad (4)$$

where  $g/RT = \beta$ , the reciprocal of the scale height. If the atmosphere is nearly isothermal, so that

$$\frac{dT}{T} \ll \frac{d\rho}{\rho}$$

(percent change in temperature with altitude is small compared to percent change in density), equation (4) reduces to

$$\frac{d\rho}{dh} = - \frac{g\rho}{RT} \quad (5)$$

which may be put in the form

$$RT = \frac{g\rho V \sin \theta}{d\rho/dt} \quad (6)$$

It follows that the local static pressure in the atmosphere may be obtained from

$$p = \rho RT = \frac{g\rho^2 V \sin \theta}{d\rho/dt} \quad (7)$$

Measured quantities are the density, rate of increase of density, instantaneous flight velocity, and flight-path angle.

Another, somewhat more direct, way to obtain the static pressure from the measurements of density is to integrate the basic barometric equation

$$dp = -\rho g dh \quad (8)$$

to obtain

$$p = \int_{\infty}^h (-\rho g) dh \quad (9)$$

Since

$$dh = -(V \sin \theta) dt, \quad (10)$$

$$p = \int_0^t (\rho g V \sin \theta) dt$$

This amounts to summing up the weight of gas above the given altitude. The differential form, equation (7), works on a local basis, first obtaining  $RT$  from local measurements of  $\rho$  and  $dp/dt$ . The integral form, equation (10), has one apparent advantage - it does not require the assumption of an isothermal atmosphere. However, this assumption is normally not a serious one, so that both methods may be of use in analyzing a set of probe data.

From an accuracy analysis, based on the assumed performance of the accelerometer cited earlier, it is concluded that pressure can be obtained more accurately than the density. This follows since in equation (10)  $\rho V$  is known more accurately than  $\rho$  (see eq. (1b)). Also, the accuracies obtainable by the two evaluation techniques (eqs. (7) and (10)) are not the same. The following table gives some calculated values.

<u>Percent error in p</u>		
<u>V/V<sub>E</sub></u>	<u>Equation (7)</u>	<u>Equation (10)</u>
1.0	2.1	2.1
.8	1.4	2.5
.5	1.5	4
.2	19	10
.1	$\begin{cases} +349 \\ -55 \end{cases}$	20

Equation (7) is the more accurate for early stages of the entry, but becomes very bad at the low velocities. The favorable error levels for equation (7) at higher velocities were calculated with the assumption that there were no random noise-type errors in the acceleration measurement - only the systematic errors described earlier. Noise would, of course, degrade the definition of the derivative  $dp/dt$  and would tend to favor the use of equation (10).

The RT product defined by equation (6) is also basically useful information. The determination of either R or T by any technique then permits the other quantity to be known also. For example, if T is measured, R may be obtained, and, in turn, the mean molecular weight

$$M.W. = \frac{Ru}{R} \quad (11)$$

of the atmospheric gases may be calculated. However, its accuracy is limited by the accuracy of R, which is approximately the same as the accuracy of p obtained by the integration method. A discussion of possible measurement techniques for obtaining atmospheric temperature will be given later.

In the above analysis no error in determining pressure was attributed to definition of  $\sin \theta$ . In both equations (7) and (10), however, the flight-path angle  $\theta$  is needed. It is also required to convert  $\rho(t)$  and  $p(t)$  to altitude profiles  $\rho(h)$  and  $p(h)$ , since time after entry is not a fundamentally important variable and what we really wish to know is the dependence of  $\rho$ ,  $p$ , etc., on altitude. The relation between time and altitude is as follows:

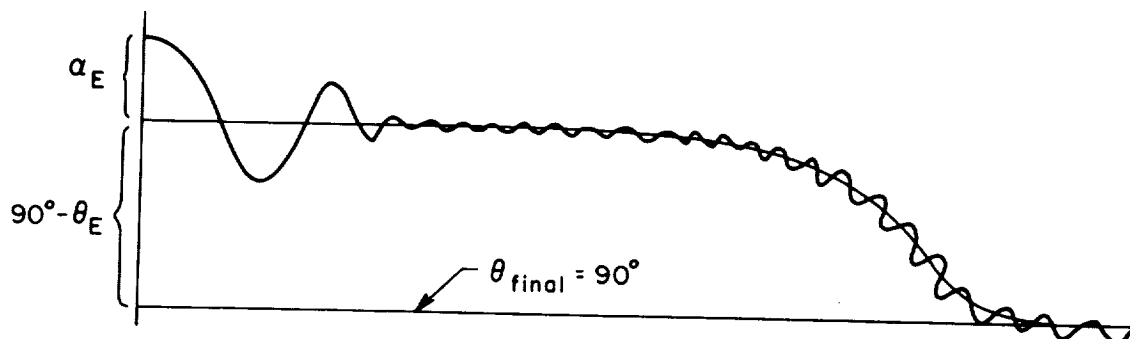
$$h = \int_t^{t_{\text{impact}}} (V \sin \theta) dt \quad (12)$$

Altitude may be calculated from the flight-path angle  $\theta(t)$  and the velocity  $V(t)$ .

One possible way of satisfying the need to know  $\sin \theta$  in equations (7), (10), and (12) is to guide the entry probe into a nearly vertical entry,  $\theta \approx 90^\circ$ , so that  $\sin \theta \approx 1$ . The actual entry angle may then depart as far as  $\pm 18^\circ$  from vertical and still introduce only 5-percent error if  $\sin \theta$  is assumed equal to 1.0. This error might be considered acceptable in equations (7), (10), and (12), in which case, a guidance system capable of bringing the probe into a vertical entry within  $\pm 18^\circ$  would be required.

A more general and perhaps more satisfactory solution to this problem would utilize the simplest possible angle sensing instrumentation in the probe. One system of this kind relies on the assumption that, regardless of entry angle,  $\theta$  approaches  $90^\circ$  near the end of flight. This tends to be true whenever the probe slows to a very low speed before impact, because the gravitational acceleration then becomes the primary cause of motion. If it can be assumed that  $\theta_{\text{final}} = 90^\circ$  and that the probe remains gas-dynamically stable until impact, then a simple gyroscope in the probe to indicate angle change from entry to impact would give the entry angle. The gyroscope would be aligned with the body axis just prior to entry, and then allowed to remain fixed in inertial space. The angle history of the probe axis relative to the gyro axis might then be like that shown in sketch (a). This system would define  $\theta_E$  and also the attitude angle and pitching frequency of the vehicle. Further study would be required to determine whether such a system would adequately fill the need for flight-path-angle data.

Another way to determine  $\theta$ , that in some respects is very attractive, is to carry on board the entry vehicle a radio altimeter. This direct measurement of



Sketch (a)

$h(t)$  (except during the time of radio transmission blackout) yields the angle of descent through the relation

$$\sin \theta = \frac{1}{V} \frac{dh}{dt} \quad (13)$$

Some estimates, which have come to the writer's attention, however, indicate that this instrumentation is excessively heavy and bulky. It is beyond the scope of the present note to judge the merit of its inclusion.

A final point in this connection should be made. It was noted that entries near  $\theta = 90^\circ$  minimize the accuracy with which  $\theta$  must be determined. The opposite is also true - flat entries near the overshoot boundary require the most precise measurement of  $\theta$ , and also can lead to "skipping" trajectories in which  $dh/dt$  is first negative, then positive, and then negative again. The determination of atmospheric pressure by equation (10) would be considerably complicated by this type of trajectory. It is felt that steep entries free of skipping are preferable for early flights, for reasons of simplicity and accuracy.

#### Studies of Gas Composition From Static Flight Stability Measurements

The gas-dynamic moments responsible for static flight stability, being the residual moments from a balance of positive and negative moments applied over the vehicle, tend to indicate with high sensitivity small changes in the distribution of pressures. Thus the stability may be affected to a considerably greater extent than the drag by changes in gas composition. One type of configuration for which this is true is shown in figure 1. The data, taken from reference 1, show that the stability derivative increases progressively as the ratio of specific heats increases. Note that the flight stability of this body in helium and argon correlates along a single curve, in spite of the large differences in molecular weight and gas constant. This indicates that the ratio of specific heats is the gas property primarily responsible for the changes in stability.

From a measurement of the Mach number and the stability derivative of this configuration (or one having similar behavior), it should be possible to estimate the mean ratio of specific heats in the planetary atmosphere. Since the Mach number  $M_\infty(t)$  is up to this point not determined, it is necessary to discuss in

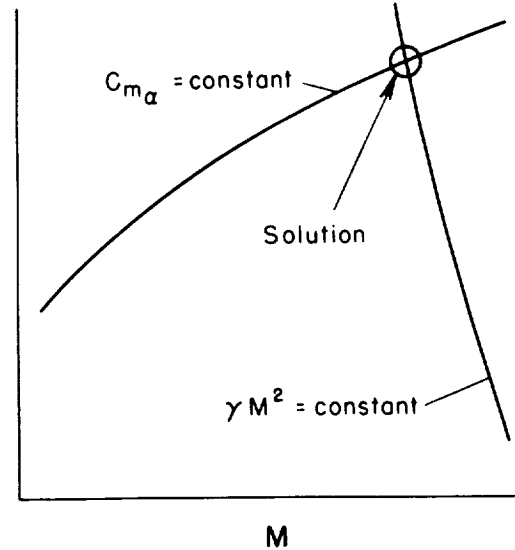
some detail how this analysis would be made. It must be done as a simultaneous solution using the experimental curves of figure 1 and a second known relation between Mach number and  $\gamma$ . Consider that a value of  $C_{m\alpha}$  has been obtained. This measurement has a locus on figure 1 which is a level line, since Mach number is unknown. Along the level line, a definite variation of  $\gamma$  with  $M$  holds, which is just a cross plot of the data in figure 1, as shown in sketch (b) by the line labeled  $C_{m\alpha} = \text{constant}$ . A second relation between  $M$  and  $\gamma$  is provided by the definition of  $M$ ,

$$M = \frac{V}{\sqrt{\gamma RT}} \quad (14)$$

Here,  $RT$  and  $V$  are known by the procedures of the previous section. Hence, we may write, for any time of the flight

$$\gamma M^2 = \text{known constant}$$

which is also plotted schematically in sketch (b). The intersection of the two curves is the solution point and gives the desired values of  $\gamma$  and  $M$  at time  $t$ . The analysis is repeated for other times. It would be expected, of course, that for an atmosphere of fixed composition, the same value of  $\gamma$  would be obtained at all times.



Sketch (b)

The stability derivative is obtained from measurements of the frequency of the attitude oscillation provided by the attitude-indicating gyroscope discussed earlier or its equivalent. The defining equation is

$$2\pi f = \sqrt{\frac{(-C_{m\alpha})(1/2)\rho V^2 A d}{I}} \quad (15)$$

which, when solved for  $C_{m\alpha}$  as a function of acceleration in the flight direction, becomes

$$C_{m\alpha} = 4\pi^2 \frac{\sigma^2}{d} C_D \frac{f^2}{a_x} \quad (16)$$

Thus, the stability derivative is given by known constants, the drag coefficient, the pitching frequency, and the axial acceleration.

Although the curves in figure 1 have, for simplicity, been labeled with the value of  $\gamma_\infty$ , ratio of specific heats in the free stream, it is well known that  $\gamma$  varies with position in high-temperature flow fields as a result of dissociation, vibration, and other chemical and thermodynamic processes. Hence, it is probably more precise to consider that every gas mixture has, at a given ambient pressure, a characteristic curve in the coordinates of figure 1. Thus, all gases

of  $\gamma_{\infty} = 1.4$  would not produce the same stability curve, because of differences in dissociation temperature, products of dissociation, etc. This may be regarded as an advantage in that it provides, in principle, a method for distinguishing between gases of the same  $\gamma_{\infty}$ . For this reason, obtaining the trace of stability as a function of Mach number over the widest possible range of Mach numbers should be valuable.

It is worth noting that attached flow over blunt-nosed slender bodies is reasonably well understood theoretically (refs. 2 and 3). The effects of gas composition on stability calculated with this theory roughly agree with measurements, although the stability derivative cannot be obtained theoretically with the precision necessary for these experiments at the present time. The theoretical understanding would, however, be of value. For example, it might be necessary to consider possible effects of nonequilibrium chemistry on the stability for gases, such as carbon dioxide, which when dissociated are very slow to recombine.

Other problems would require experimental support, notably cases involving separated flow. Also, experiments should be relied on to supply the dependence of stability on Mach number for comparison with the flight data. Additional ground-facility experiments could define these curves better for the gases which have been considered and for other gas mixtures.

It seems probable that other configurations will be found that are sensitive in static stability to gas composition. It would be particularly desirable to find a body which has this property but is not subject to flow separation effects, such as can occur on the flare of the present configuration. It may be that bodies for which the afterbody pressures are dominated by the blast-wave producing influence of a blunt nose will, in general, show some degree of  $\gamma$  sensitivity.

## OTHER MEASUREMENTS

### Atmospheric Temperature

Aside from its basic value as a property of the planet's atmosphere, the atmospheric temperature has the potentiality of leading through equation (11) to the determination of the mean molecular weight of the atmospheric gases as noted earlier. Unfortunately, the free-stream static temperature of the atmosphere has essentially no gas-dynamic effect other than to determine the free-stream Mach number. Thus, Mach number and velocity measurements used in conjunction with equation (14) would merely supply a redundant value of  $RT$  and would not assist in defining  $R$  or  $T$  separately.

Near the end of the flight, when the speed becomes subsonic, the gas temperatures are not much affected by fluid-dynamic effects and the atmosphere temperature may be measured directly to permit the determination of  $R$ . (This would require precautions to avoid measurement errors due to the presence of the hot heat shield.) At high speeds, however, this is not possible because of compression and frictional heating of the gas around the probe. It may be sufficient to defer atmospheric temperature measurements to the low-speed period and

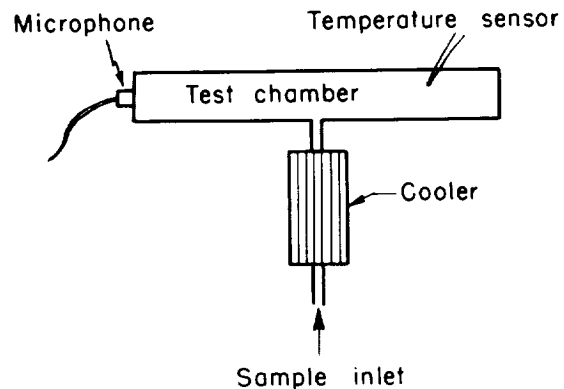
to determine the mean molecular weight only at low altitudes. It would then be reasonable to infer temperature at higher altitudes by assuming constant  $R$ , given  $RT(h)$ . Unfortunately, however, the accuracy in  $RT$  measurements deteriorates at low speeds, so that such a procedure might result in a serious loss of accuracy in determining the molecular weight.

Two techniques have occurred to the author for determining atmospheric temperature in the free stream at the higher speeds and altitudes. While they do not appear extremely attractive, the end result of determining the mean molecular weight accurately and as a function of altitude may be judged to be of such great value that these or equivalent techniques should be considered. The first is to conduct on-board experiments with a gas sample as schematically indicated in sketch (c). The gas sample is drawn through a cooler into a test chamber where (a) its temperature is measured, and (b) its sound speed is determined from the frequency of reverberation of a single pulse introduced by the microphone, which serves both to excite and to measure the vibrations. The gas constant and molecular weight are then computed from

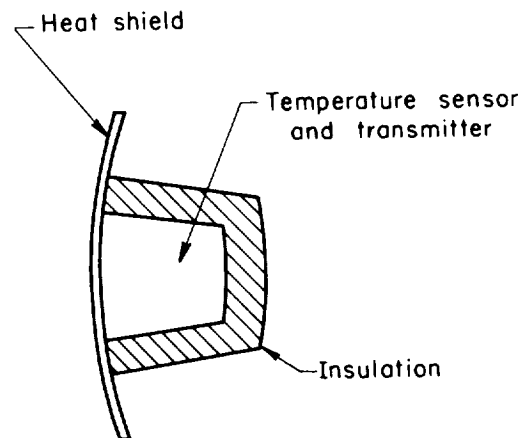
$$R = a^2/\gamma T = R_u/M.W. \quad (17)$$

A serious difficulty with this approach is the possibility of contamination of the gas sample by heat-shield ablation products, which, it is believed, would be difficult to avoid. Another source of error is the possibility of dissociated atmospheric gases being frozen in the dissociated condition while being cooled. A further problem is the small time available for readying the sample, particularly if the measurement is to be made at several altitudes, since the entire entry period is less than half a minute (see Trajectory Considerations). These considerations make this technique appear something less than promising.

A second method is to release a low-density subprobe designed to decelerate to low speed at a high altitude, to measure the static temperature directly and telemeter it to the entry probe for recording and later relay. For example, a subprobe weighing 3 pounds with a frontal area of 1 square foot and a drag coefficient of 1.5 ( $m/C_D A = 1/16$  slug/ft<sup>2</sup>) would decelerate from an entry velocity of 26,000 ft/sec to 1300 ft/sec at an altitude of 220,000 feet in the Jet Propulsion Laboratory Mars atmosphere "E." It would then take several minutes to drift down to the planet. It might have a configuration like that shown in sketch (d). A



Sketch (c)



Sketch (d)

telemetry range of 50 miles would be required from the subprobe to the probe for steep entry angles, and much of the transmission would occur after the main probe landed. Measurement error due to the elevated temperature of the subprobe heat shield could be avoided by discarding the heat shield after the subprobe slowed down. This approach, while somewhat complicated, perhaps offers a chance for determining atmospheric temperature and molecular weight profiles at high altitude.

### Shock-Layer Spectroscopy

Because of its high speed, the probe entering the atmosphere generates a shock layer of high-temperature gas that is luminous at speeds above about 13,000 ft/sec. The radiation is normally considered as a source of heat input to the capsule, but it can also provide data on the atmosphere composition. The shock compression ahead of a blunt nose performs essentially the same function as the spark, arc, or flame used in spectroscopy - it excites the constituent gases and causes them to emit characteristic radiation, which, under proper conditions, can be interpreted to indicate which gases are present.

The shock layer would be contaminated with gases evolving from the heat-shield ablation. The ablation vapor radiation has a characteristic spectrum, which depends primarily on the heat-shield materials but may depend somewhat on the atmospheric composition. It has been determined from tests at the Ames Research Center, at speeds between 20,000 and 30,000 ft/sec, that the predominant ablation product radiation for many materials is in the infrared region of the spectrum, reflecting their lower temperature, while that from the atmospheric gases peaks in the ultraviolet. Hence, it appears that contaminant radiations may be avoided by judicious selection of materials and of wavelengths for the detectors.

The effect of varying the percent of  $\text{CO}_2$  in nitrogen and carbon dioxide mixtures of about the proportions believed to occur on Mars and Venus is illustrated in figure 2. These data are from reference 1, and were obtained in the Ames pilot hypersonic free-flight facility at a mean speed of 21,500 ft/sec and an ambient pressure of 0.02 atmosphere. Although data were obtained over the spectral range from 2,000 to 10,000 Å, the points shown in this figure are from a single ultraviolet detector centered at 3,660 Å with a band width to half sensitivity of 380 Å. A very sensitive response to small amounts of carbon dioxide is indicated. Sensitivity to mixture composition is also shown by comparison of these data with data for air, given in this figure just to the left of the origin. The radiation detected here is believed to originate from cyanogen and from ionized nitrogen molecules.

The best wavelengths for detectors to perform spectroscopic analysis of a planet's atmosphere would certainly depend on the atmosphere composition assumed. For  $\text{N}_2$  and  $\text{CO}_2$  mixtures, it would appear that one detector should respond to the ultraviolet band as shown in figure 2; it should perhaps be made more selective to separate the cyanogen and the nitrogen molecule radiations. Minor constituents such as water vapor, oxygen, or argon could also be investigated by shock-layer spectroscopy. It would appear desirable also to employ one broad-band



detector to measure total luminosity for comparison with expected total luminosity. This would serve as an over-all check on the correctness of the composition, since the presence of gases other than those presently postulated might be missed in any narrow-band detector, but would be expected to affect the level of the over-all radiation. The output of the broad-band detector would necessarily be corrected for radiation from ablation products on the basis of laboratory tests such as those referred to above.

The results obtained from this kind of instrumentation would be strengthened by the fact that they produce a line trace on a map of luminous intensity as a function of speed and density, rather than an isolated point of data. The trace would be compared with a reference map obtained from laboratory tests in atmospheres of assumed composition at the flight velocities and densities. Agreement with the reference map at all times of flight would be rather convincing evidence of the correctness of the assumed composition. Furthermore, the necessity for agreement at all points of the map should assist in ruling out incorrect interpretations of the data.

### Stagnation Temperature Effects

The stagnation temperature of a gas mixture is a sensitive function of the gas composition at a given ambient pressure and total enthalpy, or equivalently, at a given flight velocity and altitude. Temperature is shown in figure 3 as a function of enthalpy for pure carbon dioxide and pure nitrogen for pressures of 0.01 atmosphere and 1 atmosphere. The data for this figure were taken from references 4 and 5. The corresponding curves of stagnation temperature as a function of flight velocity are shown in figure 4. The large variations in kinetic temperature with gas composition are noteworthy. At velocities between 10,000 and 20,000 ft/sec, stagnation temperature differences as large as  $4500^{\circ}$  R occur between these two pure gases.

Unfortunately, this gas temperature is difficult to measure. Direct measurement with thermocouples must be ruled out for  $N_2$ , and for  $CO_2$  in the early parts of the flight, because the temperatures are high enough to vaporize the sensor. The radiation measurements described above constitute a temperature measurement, in a sense, but the temperature becomes known only when the composition is established. What is desired here is an independent, more direct determination.

Ordinarily, a convective heat-transfer measurement is a way of indirectly obtaining the driving temperature potential. However, in reference 6, it is contended that heat transfer in dissociating gas systems is driven by the total enthalpy and not by the total temperature. The writer would argue that this cannot be true in the case of elevated wall temperatures, because in the limit where wall temperature equals stagnation temperature, no heat transfer due to either conduction or diffusion would be expected. Hence, the wall temperature for zero heat transfer is a strong function of the gas stagnation temperature rather than of stagnation enthalpy. For wall temperatures which are high but still below material temperature limits, important differences may be found in heat transfer for a given total enthalpy but for various total temperatures - that is, for

various gas compositions. This problem requires analysis by methods similar to those of reference 6, and hence requires extensive numerical computations on electronic computers. This was considered beyond the scope of the present paper, but would certainly be of interest as a possible method of determining gas composition from convective heat transfer measured as a function of flight velocity.

### Trajectory Considerations

For measurements of the kind considered above, the characteristics of entry trajectories are of interest and importance since they indicate the altitude range over which measurements will be made, the time period within which all data will be collected, the frequency and convergence of pitching oscillations, the accelerations to which the vehicle and the instruments will be subjected, etc. The author undertook to calculate some of these details of the trajectories using the method of Allen and Eggers, reference 7. Although this method is more approximate than some others that are available, it shows directly the effects of the principal variables and is quick and easy to apply. It is also acceptably accurate for steep-angled trajectories, which are not close to an overshoot boundary, that is, trajectories which are nearly straight-line paths. This is shown by figure 5 for some nearly vertical entries into Mars and Venus where the approximate calculations are compared with numerical integrations of the complete motion equations. Certainly the lack of knowledge of the atmospheres greatly overshadows any disagreement shown in figure 5.

The atmospheres used in these estimates were some of those selected by the Jet Propulsion Laboratory, NASA, for planetary studies, based on information given in references 8, 9, and 10. They are shown on logarithmic coordinates in figure 6 with the straight-line fairings used in the present calculations to approximate them.

Equations used to obtain the following results are given in the appendix. They were either taken from reference 7 or can be easily derived from those given in the reference.

Velocity-altitude histories are shown in figure 7 for both Mars and Venus. Values of the ballistic coefficient  $m/C_D A$ , ranging from  $1/16$  to  $6$  slugs/ft<sup>2</sup>, entry angles of  $30^\circ$  and  $90^\circ$ , and various atmospheric structures are included on this figure. For Mars, the following conclusion emerges (contingent on the correctness of these atmospheres): Unless measurements are made during the probe entry, a major part of the sensible atmosphere of the planet will not be investigated. In the worst case, the probe penetrates to an altitude of 26,000 feet before it has slowed to 1000 ft/sec, so that low-speed measurements, made from a parachute, for example, would be confined to the near vicinity of the surface. From the gas-dynamic standpoint, as can be seen from this figure, the atmosphere begins at about 300,000 feet. It will certainly be of interest and importance to explore this upper region. An alternative to using the vehicle entry for probe purposes which still permits relatively high altitude measurements is to make the vehicle very light so that it decelerates to low speed high in the atmosphere. The curve for  $m/C_D A$  of  $1/4$  indicates this method of approach.

For the Venus atmosphere, the limitation described above is not so severe. With reasonable vehicle parameters, the atmosphere could be explored by low-speed (parachute) techniques below an altitude of 170,000 feet. The region from there to 300,000 feet would again, however, be lost to this approach.

The time period of entry, as noted in the appendix, is directly proportional to the scale height of the atmosphere,  $1/\beta$ , and inversely proportional to  $V_E \sin \theta$ . The entry times are shown in very general form in figure 8 as a function of the scale height for entry angles of  $30^\circ$  and  $90^\circ$ . This plot is made for  $V_E$  of 26,000 ft/sec, but can easily be modified for any other entry speed. The times shown are between speeds of  $0.95 V_E$  and  $0.05 V_E$ . Extension of the velocity interval on either end greatly increases the time interval, but this is somewhat misleading since the principal deceleration occurs in the periods shown. For vertical entry at scale heights as small as 20,000 feet, the entry times are very short - in the neighborhood of 10 seconds. Such short times pose a requirement for the instrumentation systems that they be fast-acting. Of course, most of the instruments considered above can be made to have submillisecond response times, so perhaps the main requirement imposed by the short entry time is that all the data be tape recorded for later telemetry to earth at a more deliberate speed. The tape recording is also required for another reason - the well-known communications blackout phenomenon due to flow ionization which can be expected to occur at high speeds.<sup>1</sup>

The short entry times are naturally accompanied by high peak decelerations. These are shown for Mars entry speed in the lower part of figure 8. These values indicate that the instruments must be of good strength-to-weight ratio to remain undamaged during entry.

Calculations of the frequency and damping indicate frequencies from 1 to 10 cycles per second, and highly convergent oscillations (see equations in appendix). Bodies considered here were 2 feet in diameter. The frequency profile function, which shows the relative variation of pitching frequency with velocity during entry and which is universal within the limitations of this analysis, is shown in figure 9, and typical oscillatory amplitude variations are shown in figure 10. These calculations indicate that entries with small pitching rate at initial angles as great as  $45^\circ$  should pose no particular problems for measurement of stability.

#### CONCLUDING REMARKS

It appears that considerable information about the atmospheres of the planets could be obtained from measurements of entry probe interactions with the atmospheres. This information can be divided into two classes: one pertaining

---

<sup>1</sup>The high atmospheric temperatures - up to  $700^\circ$  K - presently believed to occur low in the atmosphere of Venus suggest that the tape-recorded data should be transmitted as rapidly as possible to the "bus" vehicle from which the probe was launched and stored there for transmission to earth. The author has been informed that the designs of electronic systems employing transistors to operate at elevated temperatures as high as  $700^\circ$  K is difficult if not impossible.

to the pressure, density, and  $RT$  product profiles in the gas above the planet surface, and the other pertaining to composition. The latter could not be defined completely or exactly, it is felt, particularly if the atmosphere is a complex mixture of gases similar to that on the earth. However, the principal constituents might be identified, the presence of some minor constituents might be investigated, and the mean molecular weight determined, which would certainly be a large gain over present knowledge.

It is evident that much work would be required in a number of areas to develop a probe of this type. Ground research would be required to aid in selecting important design variables. Instrument developments would be required, and additional error analyses would have to be made. This paper is far from complete in respect to these matters. It is hoped, however, that it will stimulate interest in the use of gas-dynamic effects for investigating the atmospheres of the planets.

Ames Research Center

National Aeronautics and Space Administration  
Moffett Field, Calif., Jan. 23, 1963

# APPENDIX A

## EQUATIONS USED FOR ESTIMATING ENTRY TRAJECTORIES

A basic equation of reference 7 which relates velocity to altitude (density) is

$$\frac{V}{V_E} = e^{-\frac{B}{2} \bar{\rho}} \quad (A1)$$

where

$$B = \frac{C_D A}{m} \frac{\rho_0}{\beta \sin \theta_E}$$

and

$$\bar{\rho} = \frac{\rho}{\rho_0} = e^{-\beta h}$$

Equation (A1) in the form

$$\bar{\rho} = \frac{2}{B} \ln \frac{V_E}{V}$$

is used to eliminate density in favor of velocity in the frequency equation, etc.

For the lower segment of an atmosphere represented by two intersecting exponential density variations

$$\begin{aligned} \bar{\rho} &= e^{-\beta_u h} & h > h_1, \rho_0 &= \rho_{0u} \\ \bar{\rho} &= e^{-\beta_l h} & h < h_1, \rho_0 &= \rho_{0l} \\ \bar{\rho} &= \frac{2}{B_l} \ln \frac{V_1}{V} + \bar{\rho}_1 & h < h_1 \end{aligned} \quad (A2)$$

where  $V_1$  and  $\bar{\rho}_1$  are conditions at  $h_1$ .

The time period of entry is

$$t = \frac{1}{\sin \theta_E} \int \frac{dh}{V}$$

which, by use of the preceding relations, can be put in the form

$$t(V) = \frac{1}{\beta V_E \sin \theta_E} \int_{V_E/V_1}^{V_E/V} \frac{d(V_E/V)}{\ln(V_E/V)} \quad (A3)$$

Equation (A3) gives the time elapsed in passing from velocity  $V_1$  to velocity  $V$ . Note that it is independent of  $m/C_D A$  and  $\rho_o$ . With the integral evaluated for  $V_1/V_E = 0.95$  and  $V/V_E = 0.05$ , equation (A3) is plotted in figure 8.

The acceleration is given by

$$a_x = \frac{C_D(1/2)\rho V^2 A}{m}$$

which can be reduced to the form

$$a_x = \beta V_E^2 \sin \theta_E \left[ \left( \frac{V}{V_E} \right)^2 \ln \frac{V_E}{V} \right] \quad (A4)$$

again independent of  $m/C_D A$  and  $\rho_o$ . The function

$$D\left(\frac{V}{V_E}\right) = \left(\frac{V}{V_E}\right)^2 \ln \frac{V_E}{V}$$

which describes the acceleration profile during entry, is plotted in figure 11.

At any altitude, the instantaneous pitching frequency is

$$f = \frac{1}{2\pi} \sqrt{\frac{(-C_{m\alpha})(1/2)\rho V^2 A d}{I}}$$

which, in terms of the above variables, can be written

$$f = F V_E \sqrt{\frac{D \beta \sin \theta_E}{d}}$$

where  $D = D(V/V_E)$  is the acceleration profile function,  $d$  is the reference length for the pitching moment, and

$$F = \frac{1}{2\pi} \sqrt{\frac{-C_{m\alpha}}{C_D} \left( \frac{d}{\sigma} \right)^2}$$

contains the aerodynamic and inertial characteristics of the model. The pitching frequency profile is just the square root of the acceleration profile and has been shown in figure 9.

For estimating the pitching amplitude variations, the pitching motion equation from reference 11 is employed

$$\frac{\alpha}{\alpha_E} = \left(\frac{V_E}{V}\right)^{\xi/2C_D} J_0 \left[ 4 \left(\frac{d}{\sigma}\right)^2 \left( - \frac{C_{m\alpha}}{C_D} \right) \frac{\ln(V_E/V)}{\beta d \sin \theta_E} \right]^{1/2}$$

where  $J_0$  is the zero-order Bessel function and  $\alpha_E$  is the angle of attack at entry. For present estimates, the aerodynamic damping function

$$\xi = C_D - C_{L\alpha} + (C_{mq} + C_{m\dot{\alpha}})(d/\sigma)^2$$

was taken equal to zero. This function is strongly dependent on configuration, taking on both positive and negative values, but does not greatly influence the angle history until low velocities are reached, near the end of flight (see refs. 11 and 12).

After the second positive peak of the Bessel function, which occurs at  $J_0(x) = 0.300$ ,  $x = 7.0$ ,  $V/V_E \approx 0.99$ , the following approximation for the amplitude of pitching holds

$$\frac{\alpha}{\alpha_E} = 0.300 \left(\frac{V_2}{V}\right)^{\xi/2C_D} \left[ \frac{\ln(V_E/V_2)}{\ln(V_E/V)} \right]^{1/4}$$

$V_2$  being the exact value of velocity at the second positive peak of the Bessel function.

## REFERENCES

1. James, Carlton S., and Smith, Willard G.: Experimental Studies of Static Stability and Radiative Heating Associated With Mars and Venus Entry. Presented at I.A.S. 31st Annual Meeting, New York, Jan. 21-23, 1963.
2. Seiff, Alvin, and Whiting, Ellis: The Effect of the Bow Shock Wave on the Stability of Blunt-Nosed Slender Bodies. NASA TM X-377, 1960.
3. Whiting, Ellis E., and Carros, Robert J.: Free-Flight Investigation of the Static Stability and Aerodynamic Drag of Three Blunt-Nosed Cylinder-Flare Test Bodies at Mach Numbers From 13 to 17. NASA TM X-500, 1961.
4. Ahtye, Warren F., and Peng, Tzy-Cheng: Approximations for the Thermodynamic and Transport Properties of High-Temperature Nitrogen With Shock-Tube Applications. NASA TN D-1303, 1962.
5. Raymond, J. L.: Thermodynamic Properties of the Atmosphere of Venus. Rand Rep. RM 2292, 1958.
6. Fay, J. A., and Riddell, F. R.: Theory of Stagnation Point Heat Transfer in Dissociated Air. Jour. of Aero. Sci., vol. 25, no. 2, Feb. 1958, pp. 73-85, 121.
7. Allen, H. Julian, and Eggers, A. J., Jr.: A Study of the Motion and Aerodynamic Heating of Ballistic Missiles Entering the Earth's Atmosphere at High Supersonic Speeds. NACA Rep. 1381, 1958.
8. Schilling, G. F.: Extreme Model Atmospheres of Mars. RM 402-JPL, Aug. 1962.
9. Spiegel, Joseph M.: Effects of Mars Atmospheric Uncertainties on Entry Vehicle Design. Aerospace Engr., vol. 21, no. 12, Dec. 1962, pp. 62-3, 103-7.
10. Kaplan, Lewis D.: A Preliminary Model of the Venus Atmosphere. Tech. Rep. 32-379, JPL, Dec. 1962.
11. Allen, H. Julian: Motion of a Ballistic Missile Angularly Misaligned With the Flight Path Upon Entering the Atmosphere and Its Effect Upon Aerodynamic Heating, Aerodynamic Loads, and Miss Distance. NACA TN 4048, 1957.
12. Sommer, Simon C., and Tobak, Murray: Study of the Oscillatory Motion of Manned Vehicles Entering the Earth's Atmosphere. NASA MEMO 3-2-59A, 1959.



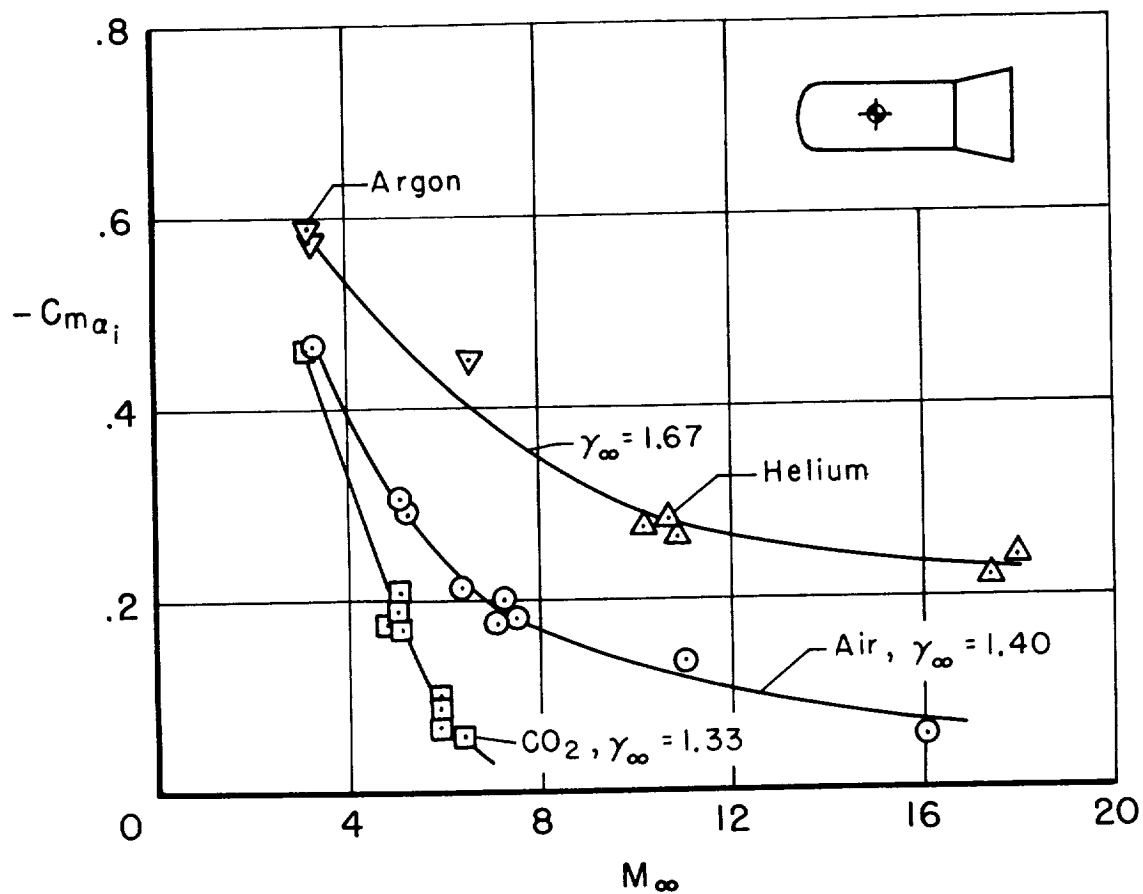


Figure 1.- Data from reference 1 showing the sensitivity of static stability to  $\gamma$  for blunt-nosed flare-stabilized bodies.

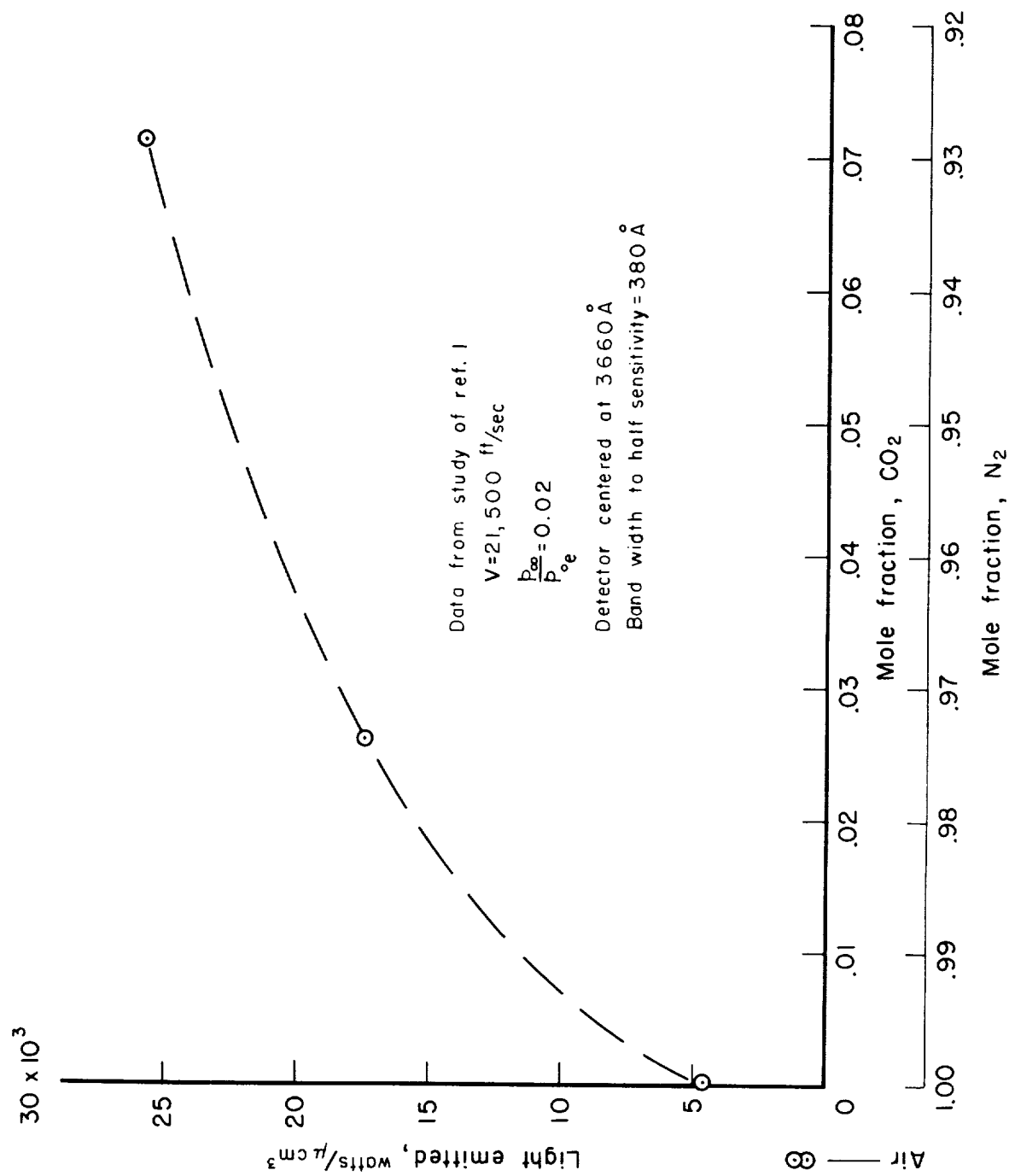


Figure 2.- Light emitted near  $3700 \text{ \AA}$  wavelength per cubic centimeter of gas in the shock layer as a function of amount of CO<sub>2</sub> in N<sub>2</sub>-CO<sub>2</sub> mixtures.

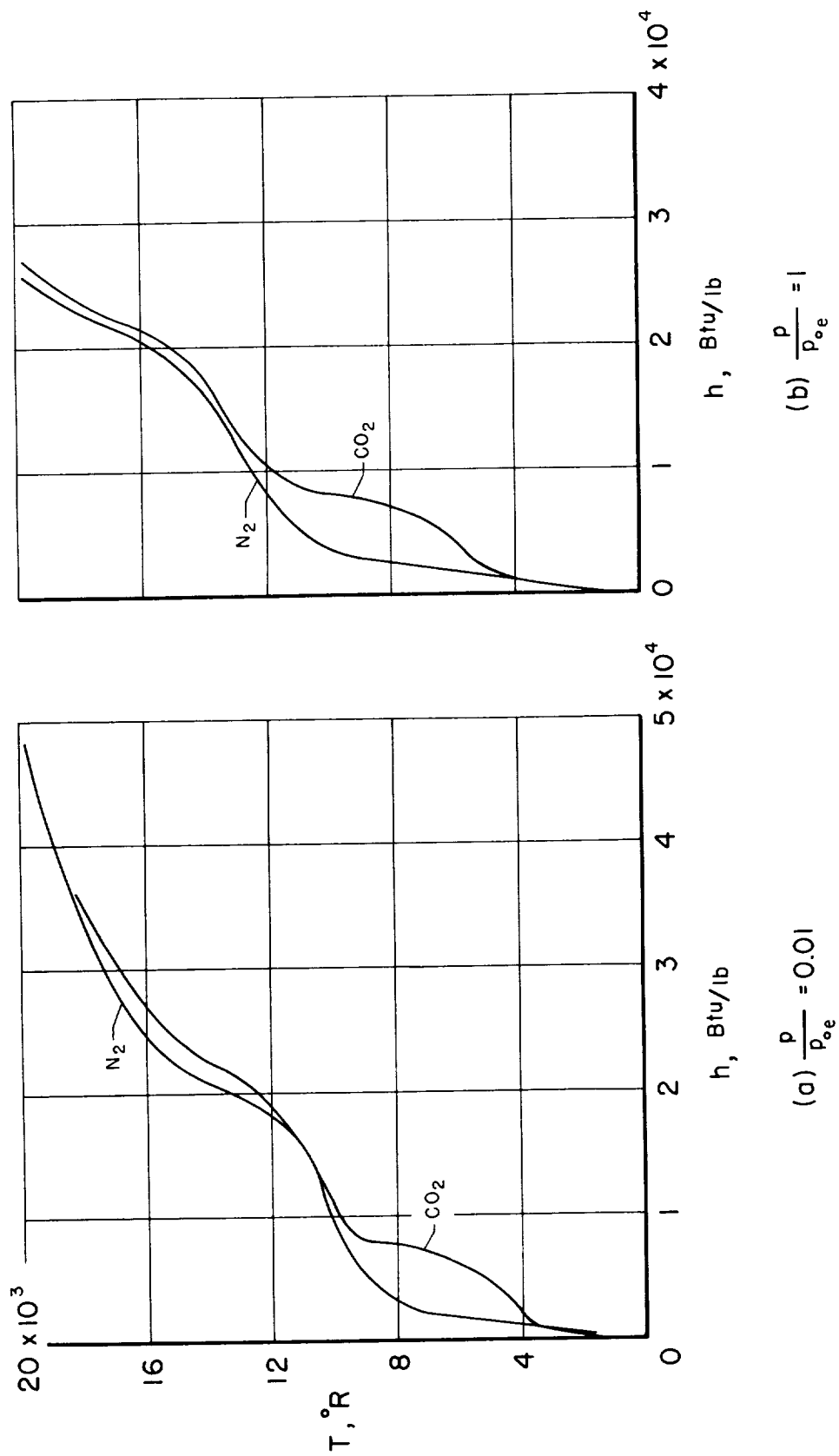


Figure 3.0.- Temperature as a function of enthalpy for pure  $\text{N}_2$  and pure  $\text{CO}_2$ .

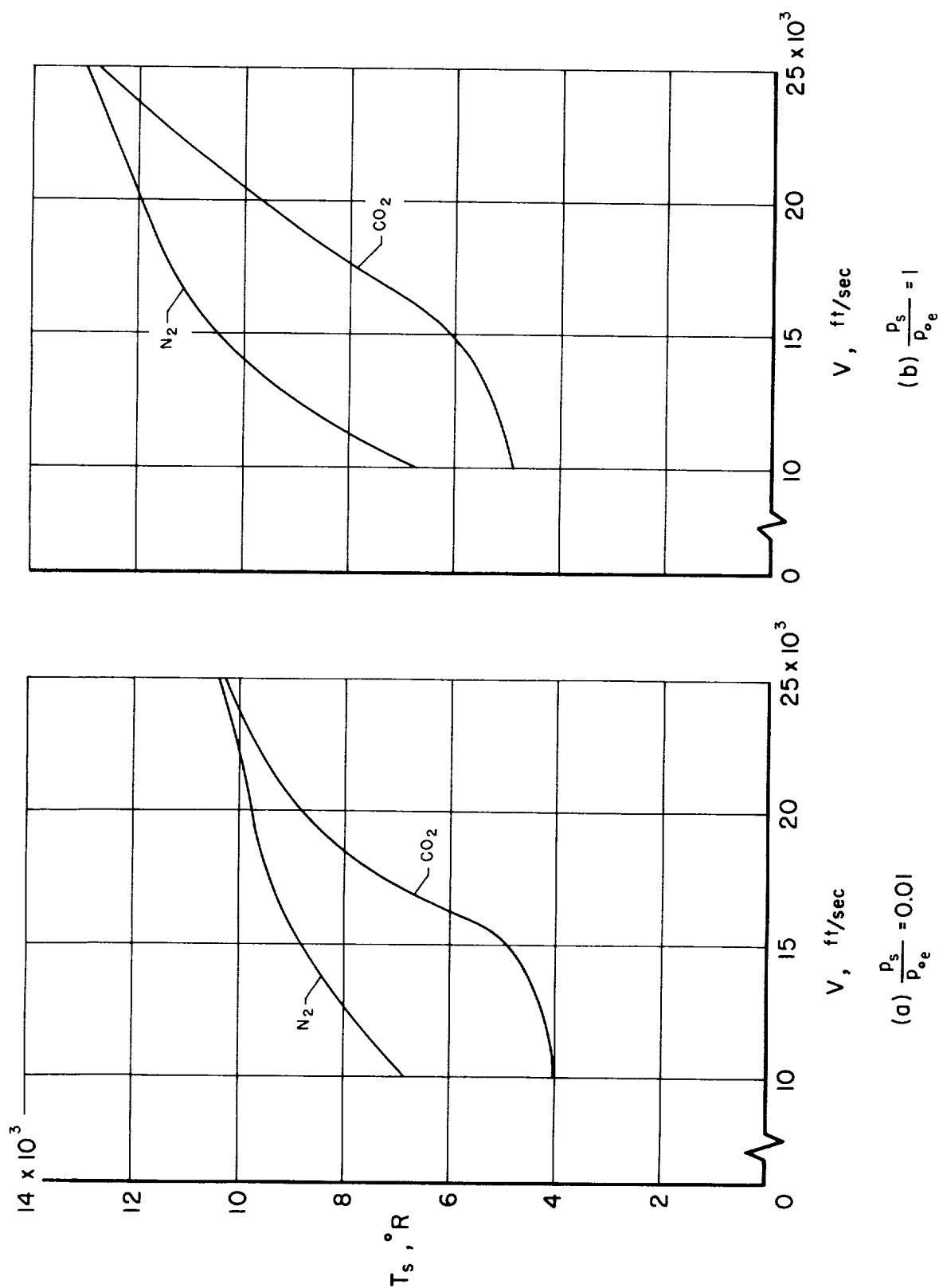


Figure 4.- Stagnation temperature as a function of flight velocity for pure  $N_2$  and pure  $CO_2$ .

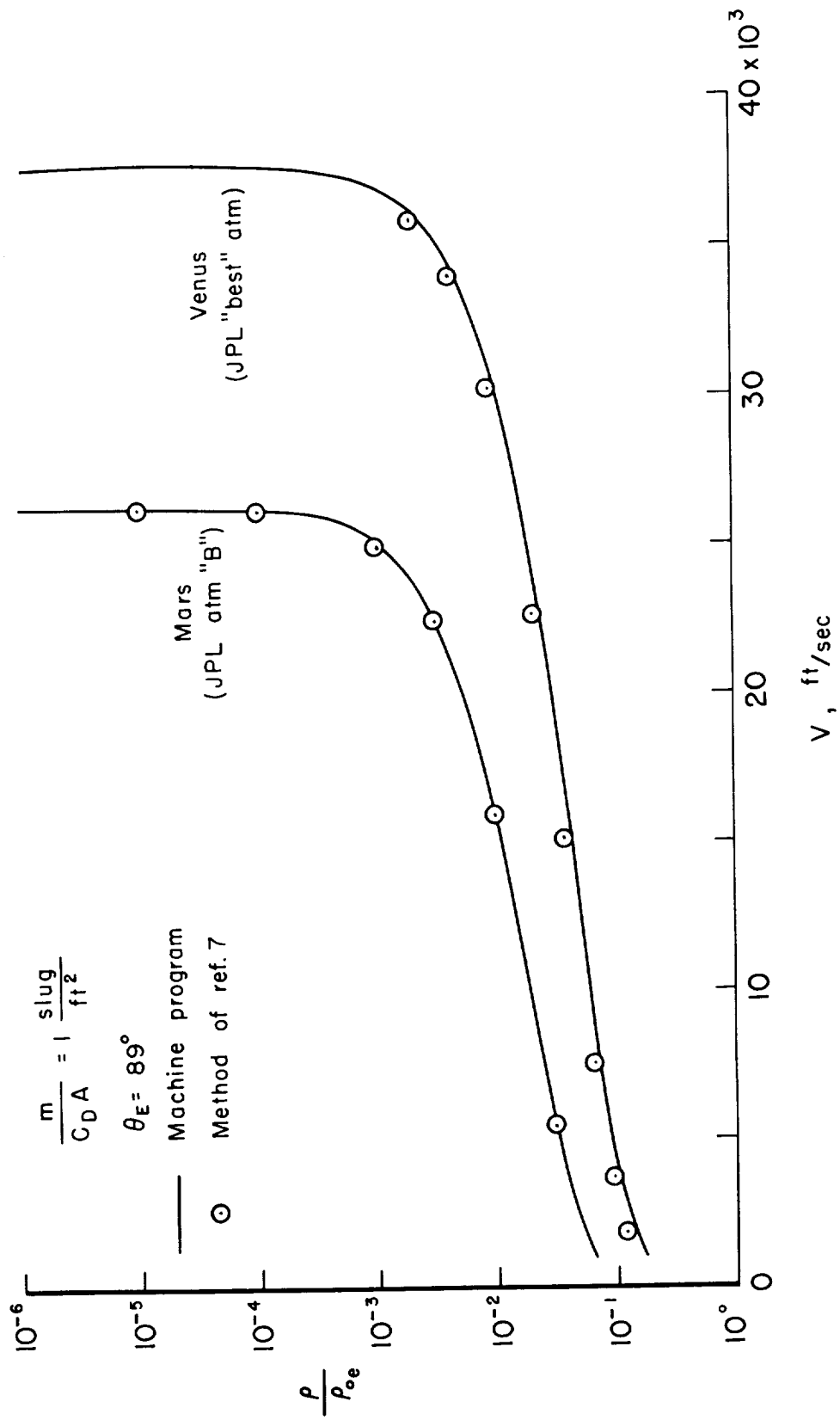


Figure 5.- Comparison of machine-program trajectories with method of reference 7 for nearly vertical entries.

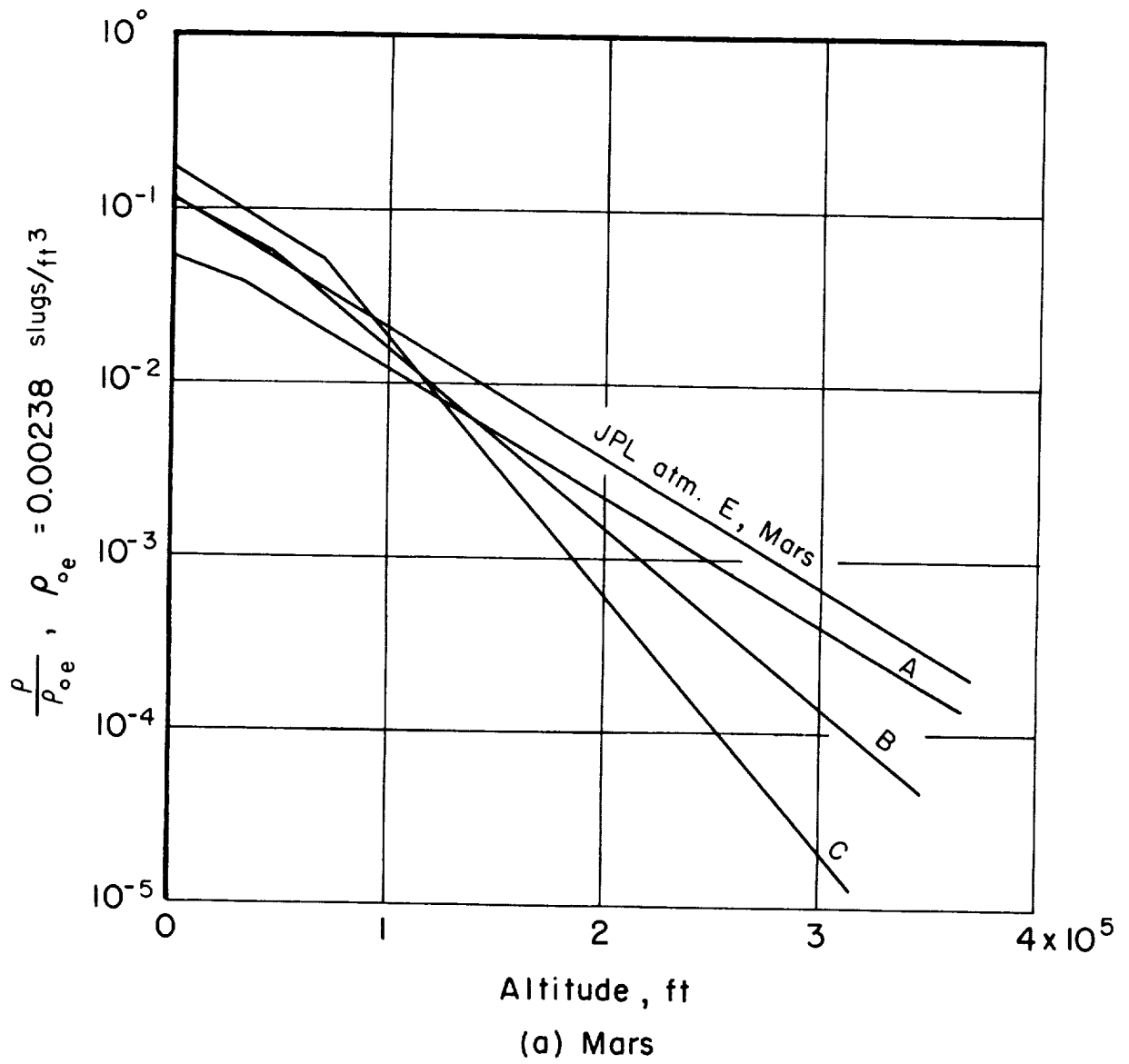


Figure 6.- Model atmospheres used for trajectory calculations.

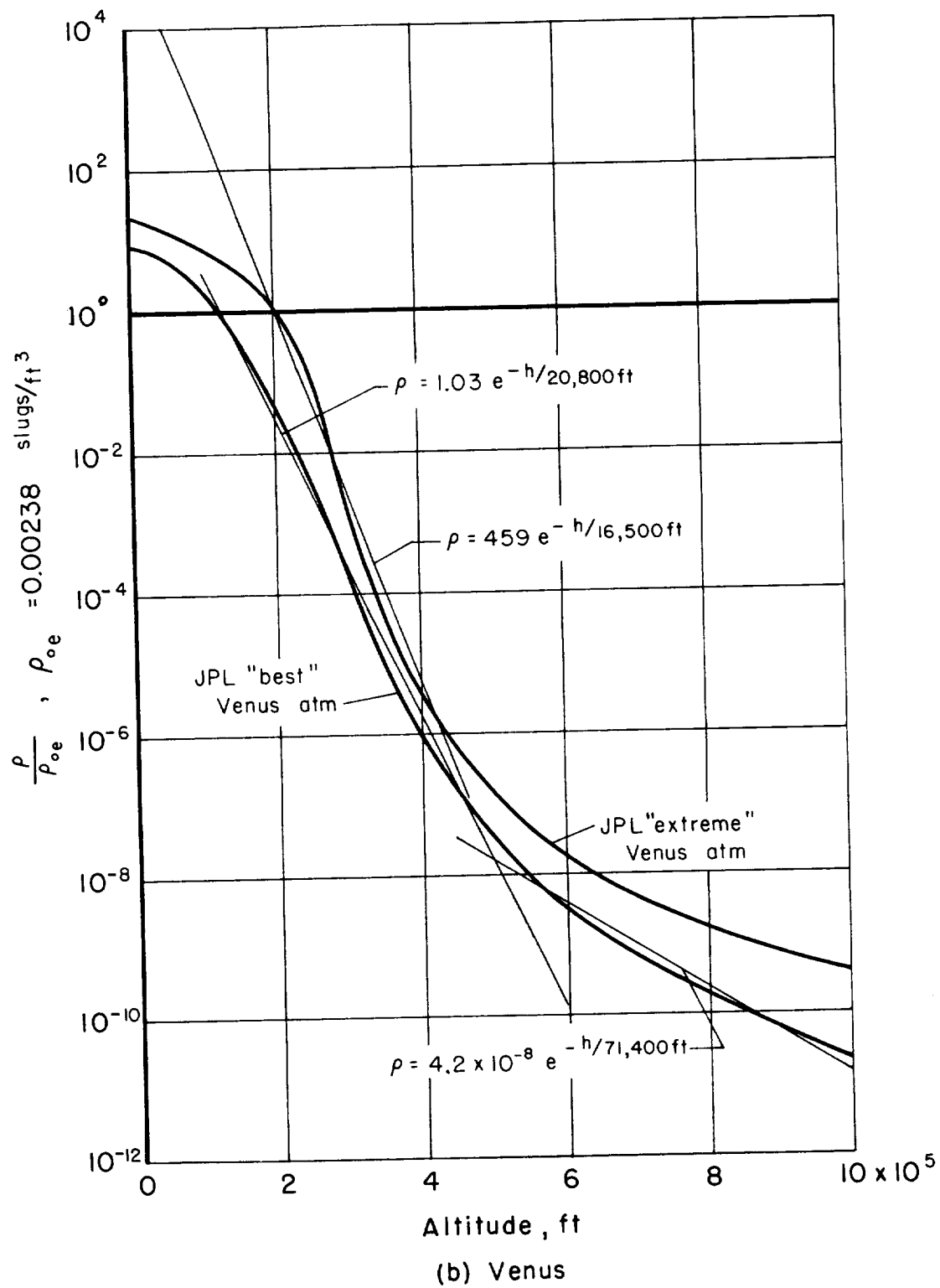


Figure 6.- Concluded.

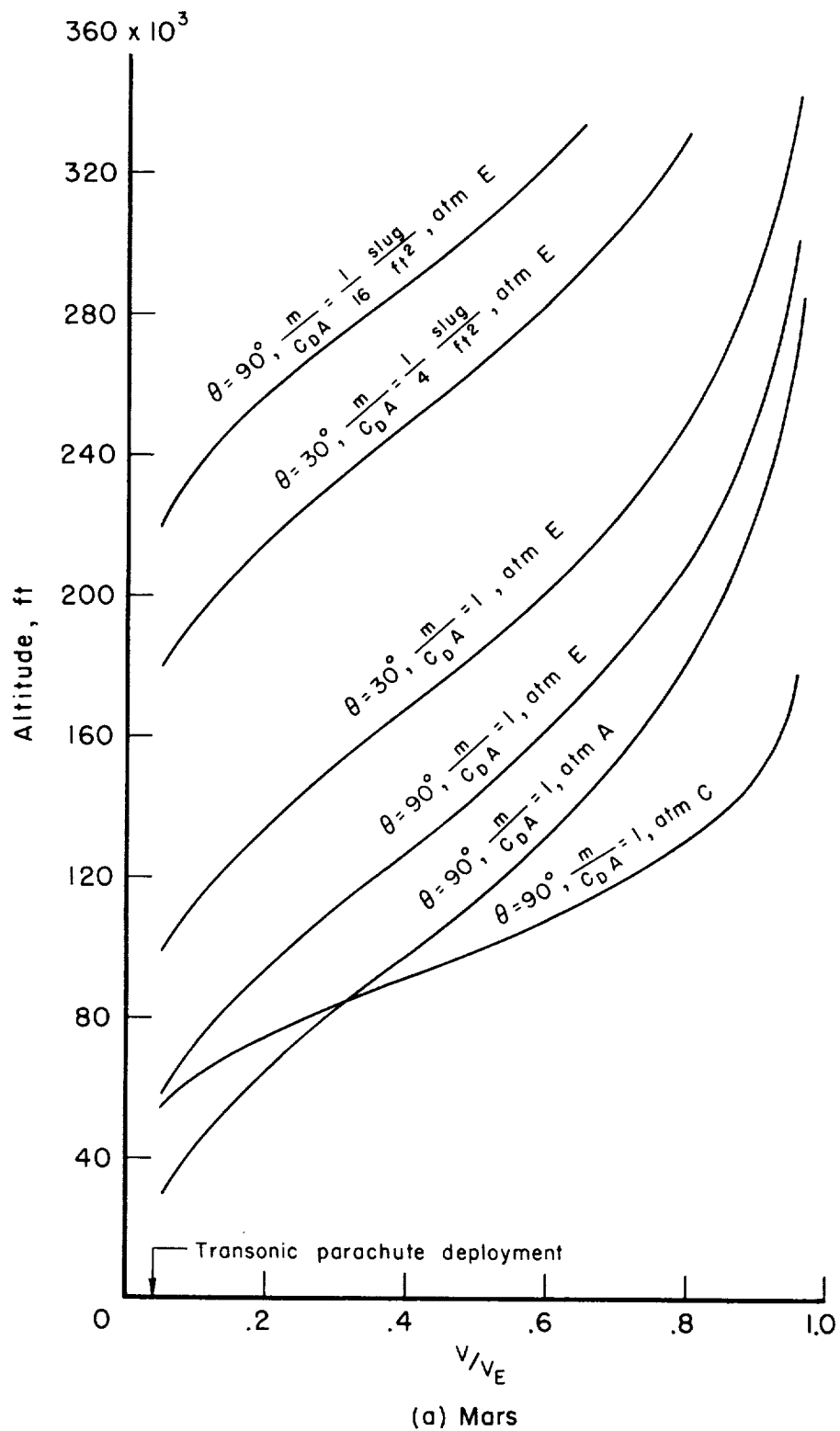
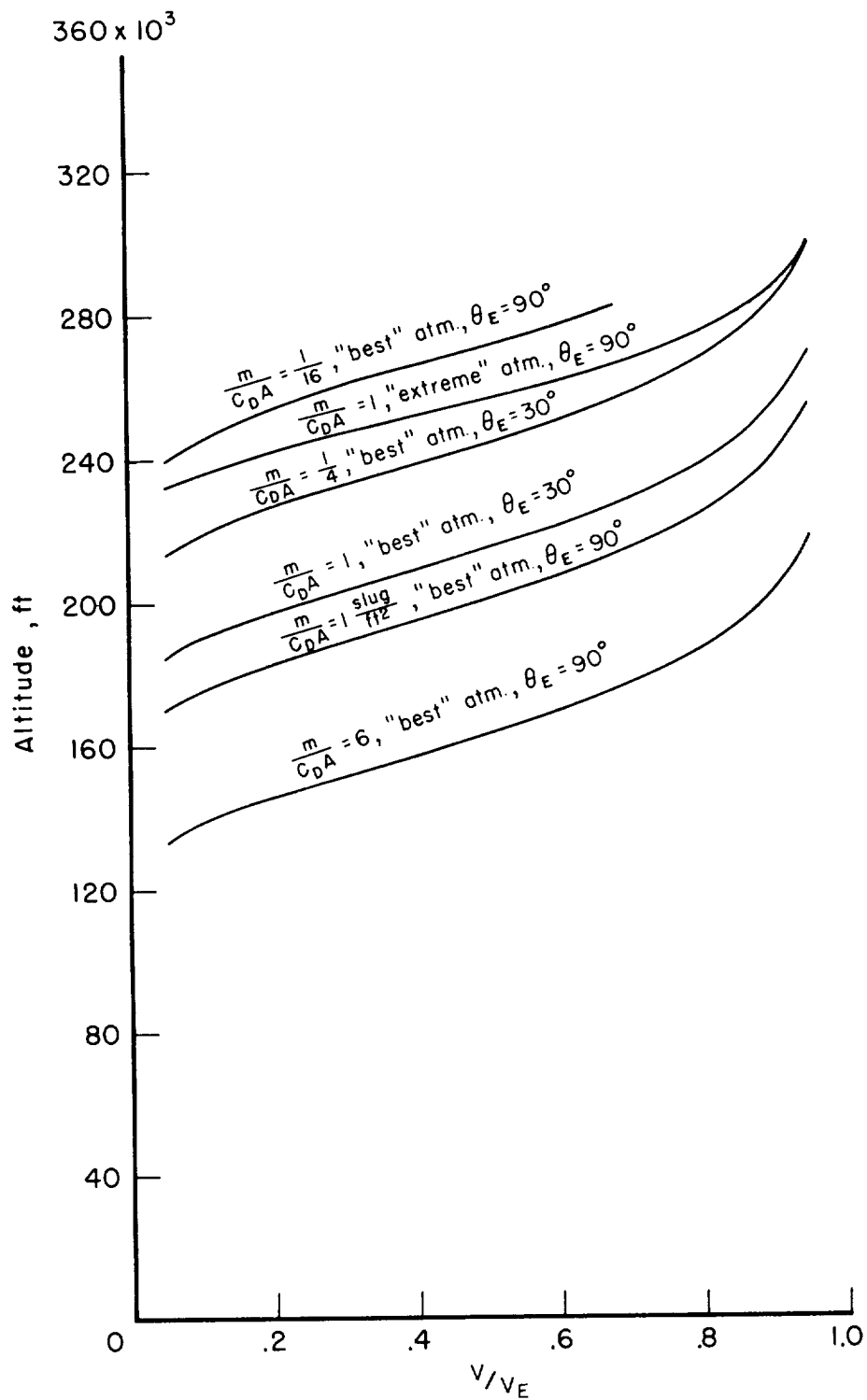


Figure 7.- Altitude-velocity relations.





(b) Venus

Figure 7.- Concluded.

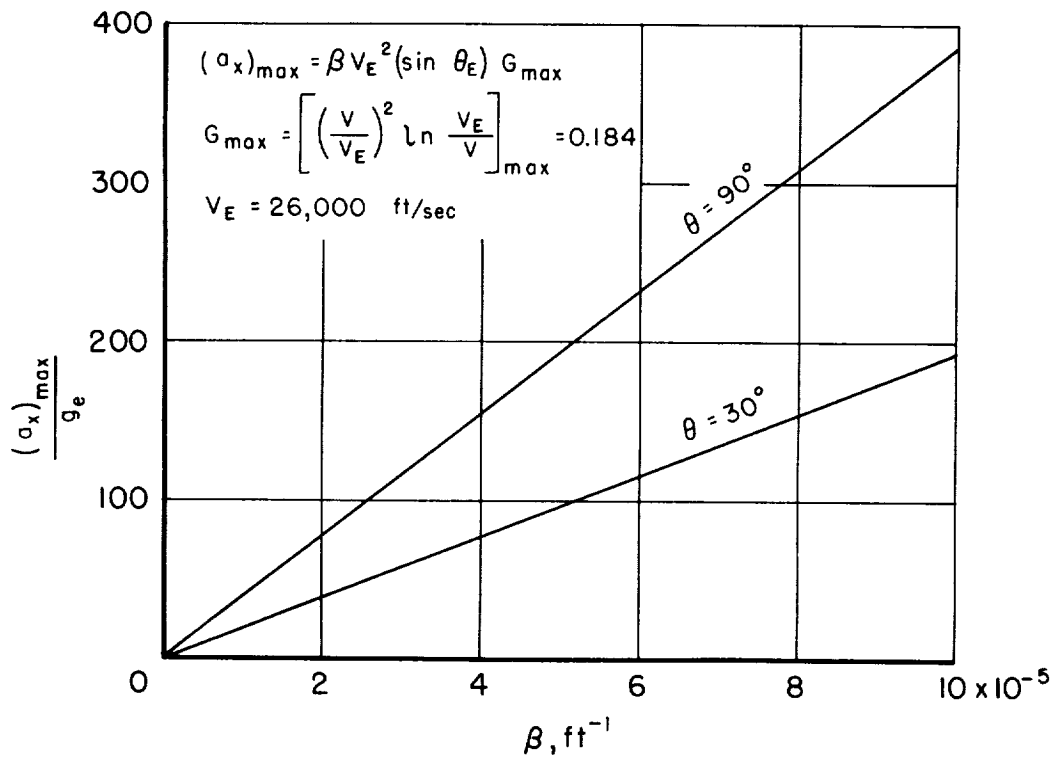
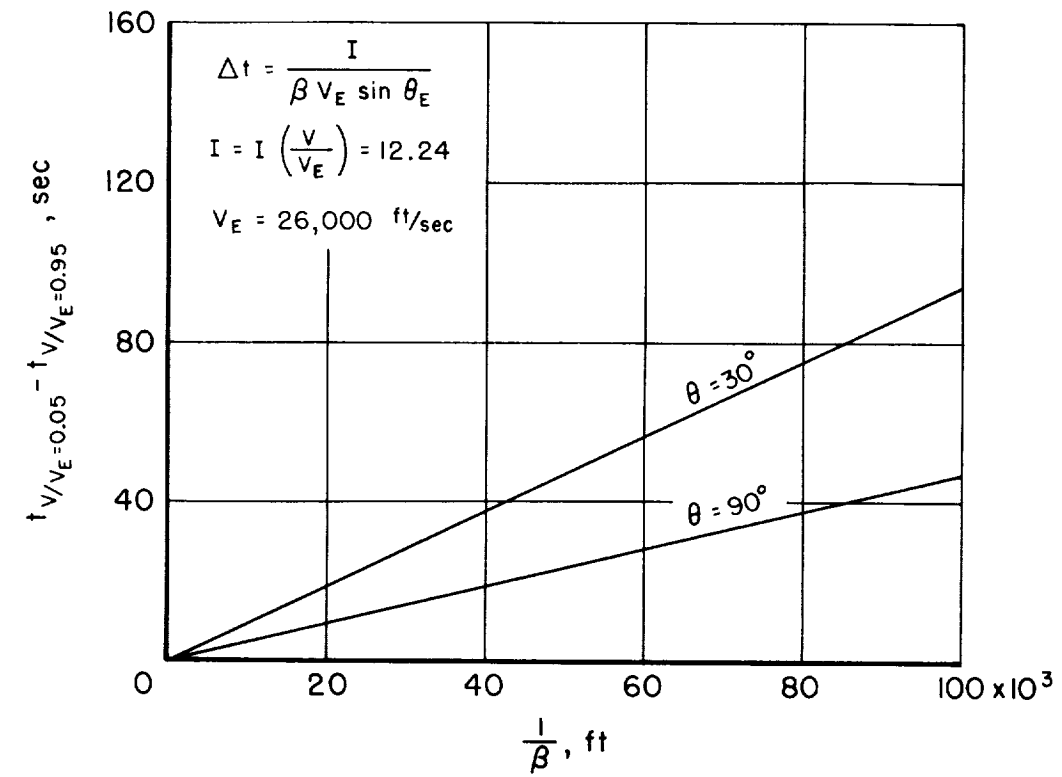


Figure 8.- Time duration of entry and peak acceleration.

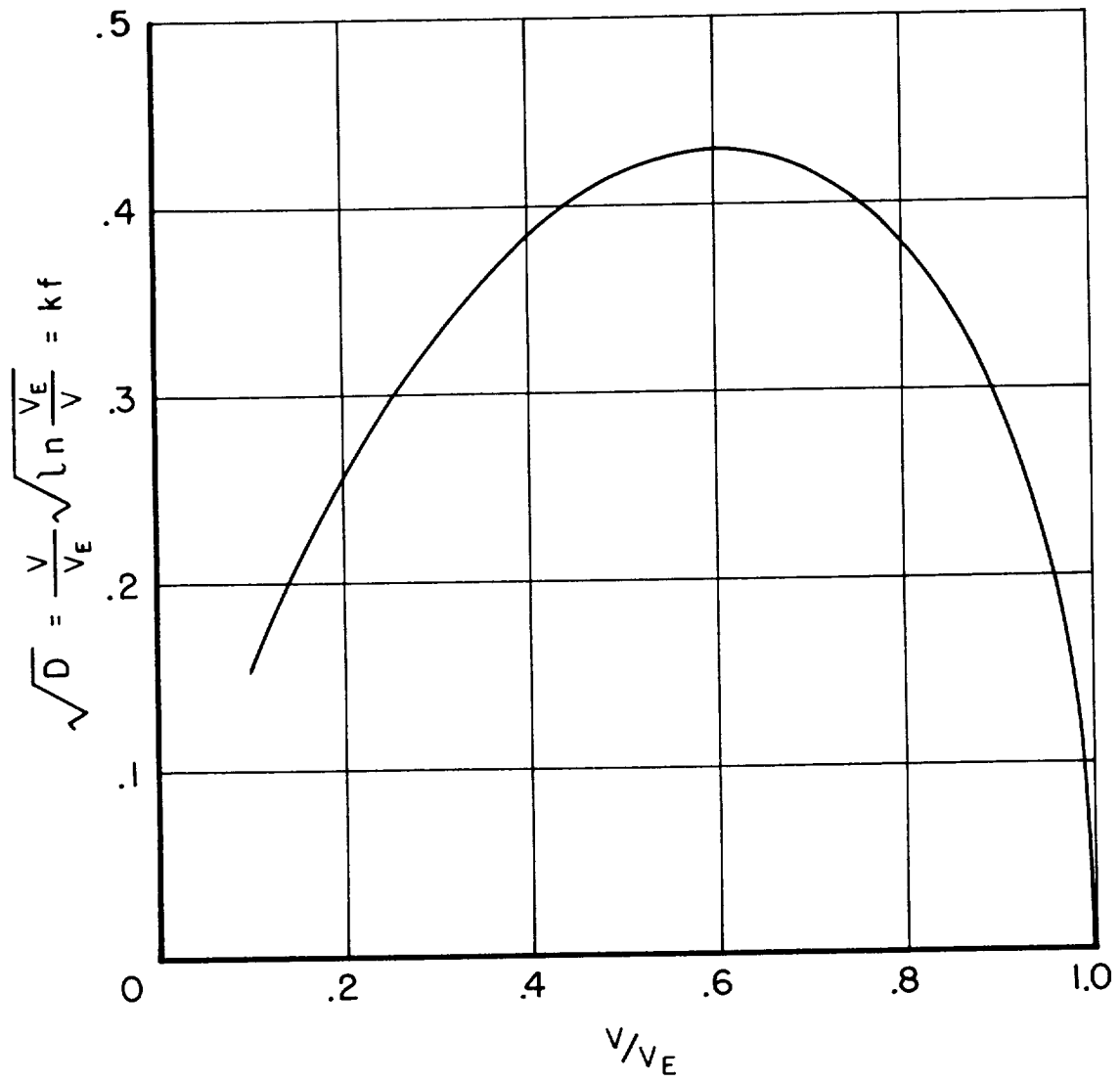


Figure 9.- Frequency profile function.

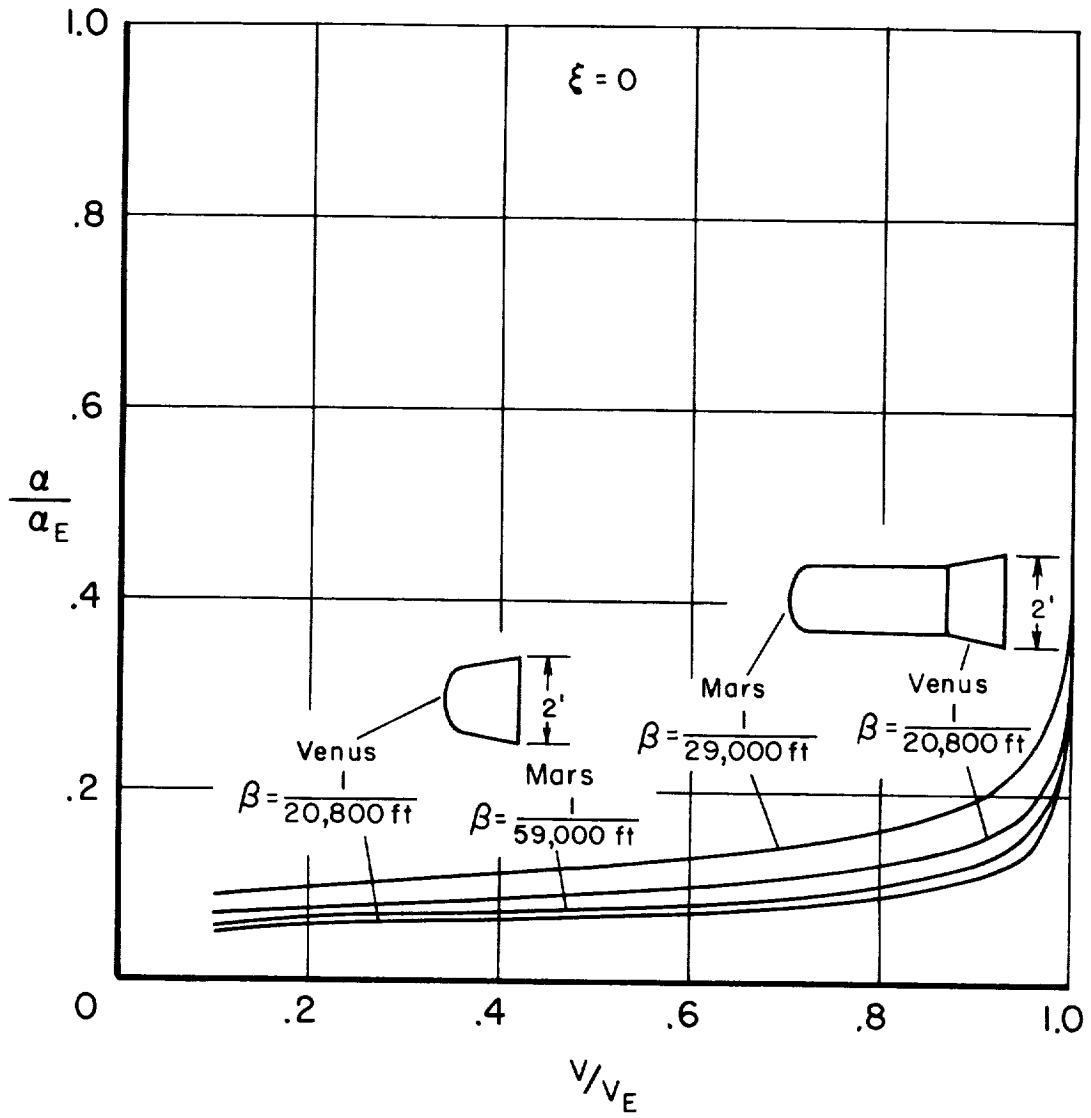


Figure 10.- Amplitude convergence on Mars and Venus entries.

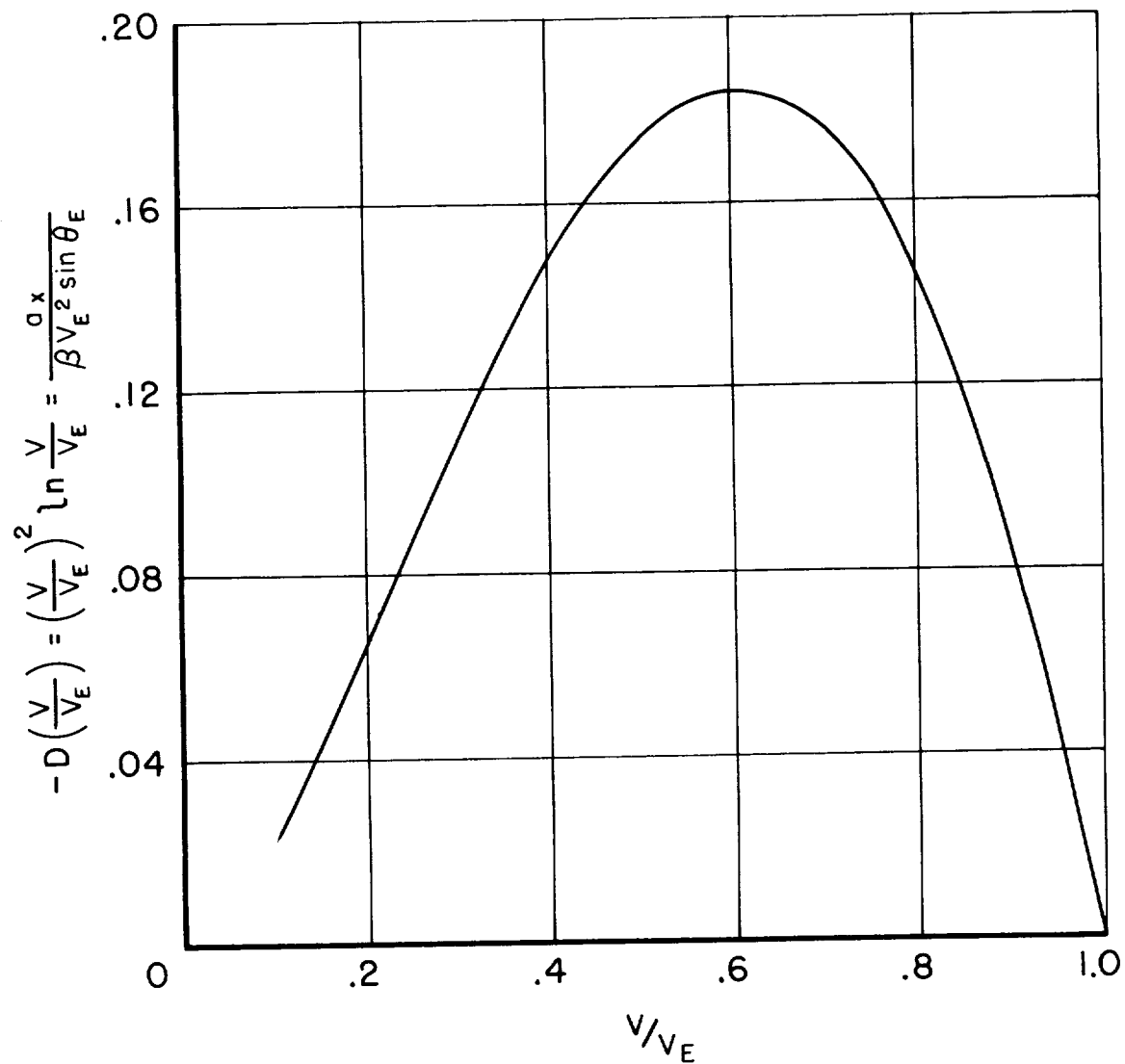


Figure 11.- Acceleration profile function.





